

## TOLERANCE ANALYSIS OF A 500 GHz AMPLITUDE HOLOGRAM

Taavi Hirvonen, Jussi Tuovinen, Antti V. Räsänen,  
Radio Laboratory, Helsinki University of Technology,  
Otakaari 5A, FIN-02150 Espoo, Finland

### ABSTRACT

The antenna of the Odin satellite is planned to be tested with a hologram type of a compact antenna test range (hologram CATR) at 119 GHz and 500 GHz. The quiet-zone field is analysed theoretically by using an exact near-field aperture integration method. Main focus of this paper is on the hologram pattern errors parallel to the surface of the hologram. Also the surface flatness requirement is discussed. Due to fabrication errors the slots of the hologram are wider or narrower than in an ideal case, which is shown as increased amplitude and phase ripple in the quiet-zone. Large holograms have to be fabricated by joining several pieces together. A possible displacement of the pieces causes an inclination to the amplitude and phase in the quiet-zone. Also the effect of a frequency change has been simulated; the effect is the inclination of the phase, i.e., the plane wave leaves the hologram in a different angle than at the design frequency.

### INTRODUCTION

Odin is an international, mainly Swedish satellite project for monitoring aeronomical and astronomical spectral lines. On the astronomy side the main purpose of the satellite is to perform detailed studies of the physics and the chemistry of the interstellar medium by observing emission from key species. The main targets for observations are giant molecular clouds, nearby dark clouds, comets, planets, circumstellar envelopes and nearby galaxies. Molecular lines of Cl, H<sub>2</sub><sup>18</sup>O, H<sub>2</sub>O, H<sub>2</sub>S, NH<sub>3</sub>, H<sub>2</sub>CO, O<sub>2</sub>, CS, <sup>13</sup>CO, H<sub>2</sub>CS, SO and SO<sub>2</sub> are of interest. On the aeronomy side the stratospheric ozone depletion and the vertical exchange of green house effect gases are of interest. Molecular lines of ClO, CO, NO<sub>2</sub>, N<sub>2</sub>O, H<sub>2</sub>O<sub>2</sub>, HO<sub>2</sub>, H<sub>2</sub>O, H<sub>2</sub><sup>18</sup>O, NO, N<sub>2</sub>O, HNO<sub>3</sub>, O<sub>3</sub> and O<sub>2</sub> will be observed by limb sounding.

The Odin satellite will carry on board a millimeter and submillimeter wave radio telescope and an optical spectrometer. The radio telescope has an offset reflector antenna. The main reflector diameter is 1.1 m. This antenna is meant to operate with heterodyne receivers at frequencies 119, 422, 488, 553 and 575 GHz. The antenna is planned to be tested with a hologram type of a compact antenna test range (hologram CATR).

In this paper, the idea of a hologram CATR is described and the manufacturing process of the hologram is explained. Also the theoretical basis and the results of the tolerance analysis are presented. In this case the tolerance analysis includes the effect of the fabrication error of the hologram pattern on the field in the quiet-zone. Also, the effect of the displacement of the different parts of the hologram when the hologram is joined together from two pieces is analyzed. The analysis is based on an exact near-field aperture integration method.

## A HOLOGRAM CATR

A hologram is an interference pattern of two wave fronts. One of the interfering wave fronts can be recreated by illuminating the hologram with the other one of the original fields. The idea of a hologram CATR is described in reference [1]. Figure 1 shows the principle of the hologram CATR. The feed horn transmits a spherical wave, which is transformed into a plane wave with a planar, computer generated amplitude hologram structure. The antenna under test (AUT) is illuminated with this plane wave. The area where the plane wave meets its requirements is called the quiet-zone and it has to be larger than the antenna under test. The quality of the quiet-zone is characterized by the amplitude and phase ripple, amplitude and phase taper, crosspolarization level, spurious reflections and multiple reflections in the area [2]. In this paper, the amplitude and phase ripple as well as the amplitude and phase taper are considered.

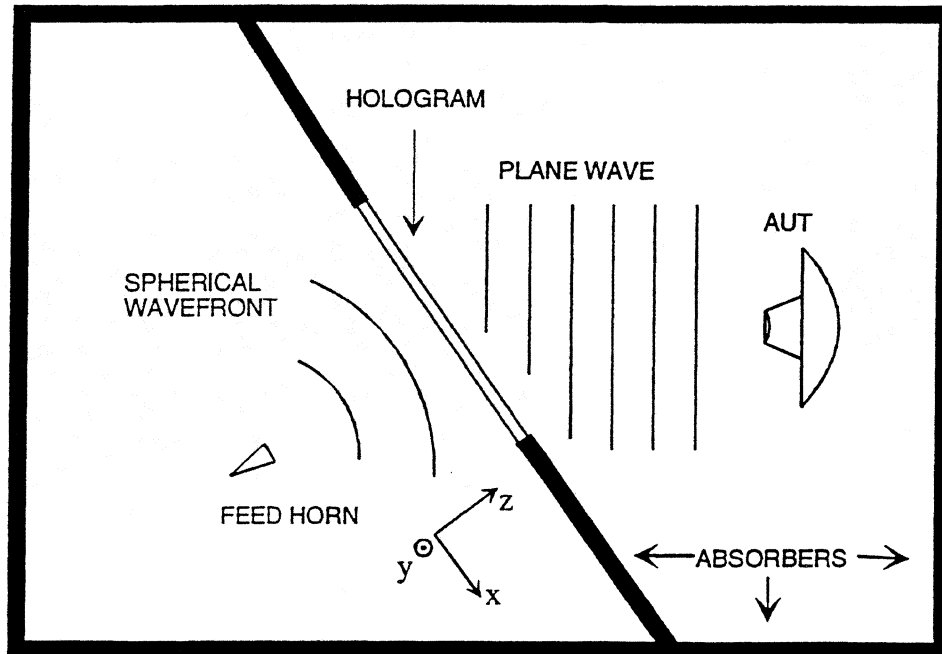


Figure 1. A hologram type of a compact antenna test range.

## FABRICATION OF THE HOLOGRAM

In many practical applications holograms are synthesized by computational methods (computer generated hologram, CGH). The hologram pattern is determined by calculating numerically the structure required to change the known input field (feed horn) into the desired output field. Due to fabrication limitations, the structure of the hologram has to be quantized in some way. This is called the coding scheme of the CGH. The two most widely used schemes are the binary phase and the binary amplitude quantizations, in which either the phase or amplitude transmittance (or reflectance) of the hologram is limited to have only two different discrete values. Different coding techniques have been reviewed in reference [3].

The discretized pattern of the hologram is printed on a film with a high precision plotter. This film is used as a mask when the pattern is transferred to a copper plated dielectric sheet covered with a photoresist. Finally, the extra copper is removed with a wet chemical etching process. The manufacturing procedure is similar to that used for making printed circuits. The manufacturing errors which affect the field in the quiet-zone are due to inaccuracies of the plotter, pattern transfer and etching. In this case the inaccuracy of the plotter is about 7  $\mu\text{m}$ . The inaccuracy of the pattern transfer is 5–10  $\mu\text{m}$  with collimated light and 50–100  $\mu\text{m}$  with uncollimated light. Usually the thickness of the copper layer is a good estimation for the inaccuracy of the etching process. A dielectric sheet with a 5  $\mu\text{m}$  copper layer is available. Therefore, the achievable inaccuracy of the widths of the slots of the hologram is about 40–200  $\mu\text{m}$  depending on the pattern transfer.

## THEORETICAL ANALYSIS OF A HOLOGRAM CATR

The transmittance of an amplitude hologram is [3,4]

$$T(x', y') = \frac{1}{2} [1 + a(x', y') \cos \Psi(x', y')], \quad (1)$$

where  $a(x', y')$  is the relation between the output and input amplitudes so that the hologram compensates the amplitude variation of the input field and adds a cosine amplitude taper to the amplitude of the output field. The phase term is  $\Psi(x', y') = \varphi(x', y') + 2\pi\nu x'$ , where  $\nu$  denotes the spatial carrier frequency, which separates the diffraction orders produced by this hologram. The desired output field leaves the hologram in an angle of

$$\theta = \arcsin(\nu\lambda). \quad (2)$$

The normalized phase of the input field (feed horn) in the plane of the hologram is  $\varphi(x, y)$ . The coordinates in the plane of the hologram are  $x'$  and  $y'$ . The transmittance of the corresponding binary-amplitude coded hologram is given by the formula

$$T_B(x', y') = \begin{cases} 0, & 0 \leq \frac{1}{2}[1 + \cos \Psi(x', y')] \leq b, \\ 1, & b \leq \frac{1}{2}[1 + \cos \Psi(x', y')] \leq 1, \end{cases} \quad (3)$$

where  $b = 1 - (1/\pi) \arcsin a(x', y')$ . In this case, the desired output field is a plane wave with a cosine amplitude taper and the plane wave is designed to leave the hologram in an angle of  $33^\circ$ . In binary-amplitude coding, the phase is stored in the locations of the slots and the amplitude information is recorded in the variations of slot widths. The main effect of the binarization is the redistribution of energy between the various diffraction orders of the hologram [5]. Figure 2 shows an example of a binary amplitude hologram.

The field in the quiet-zone is calculated by using an exact near-field aperture integration (physical optics). The formula for the quiet-zone field is [6,7]

$$\mathbf{E}(x, y, z) = \iint_S E_a \frac{1 + jkR}{2\pi R^3} e^{-jkR} [\mathbf{u}_y(z - z') - \mathbf{u}_z(y - y')] dS', \quad (4)$$

where  $R = \sqrt{(x - x')^2 + (y - y')^2 + (z - z')^2}$  is the distance from a point in the aperture (hologram) to a point in the quiet-zone. In this case, the aperture field is  $E_a(x', y') = T_B(x', y')E_{\text{feed}}(x', y')$ , where  $E_{\text{feed}}(x', y')$  is the complex field of the feed horn in the plane of the hologram. In this analysis, the aperture field is assumed to be linearly polarised in  $\mathbf{u}_y$ -direction. However, the polarization effects of a hologram structure are not included in these analyses, i.e., the incoming wave is only modulated by a scalar  $T_B$  function.

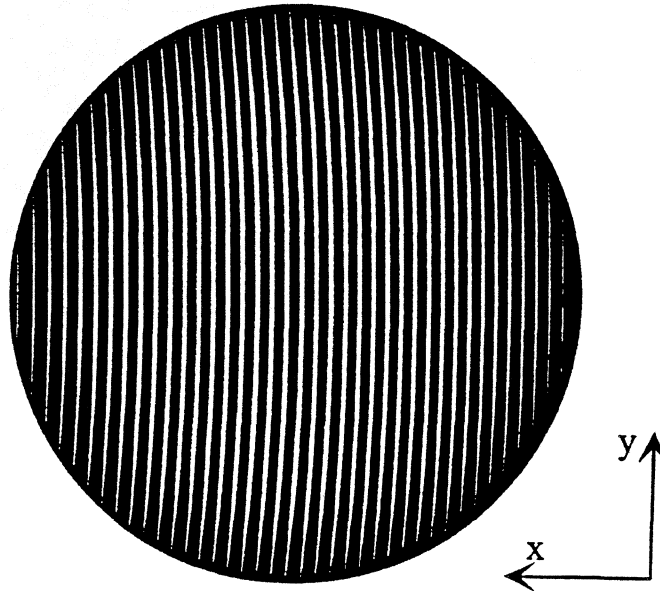


Figure 2. An example of a binary amplitude hologram.

## RESULTS

In order to keep the simulation time reasonable, the diameter of the hologram in these analyses was 200 mm at 500 GHz. Cray X-MP EA/464 and Silicon Graphics Onyx were used in the analyses. The grid spacing in the numerical integration was  $20 \mu\text{m}$  ( $\approx \lambda / 30$ ), which was found to be small enough. All the results in this paper have been calculated for the angle of  $33^\circ$  and the distance of 500 mm from the center of the hologram. Also, the results that are shown here are calculated in the  $xz$ -plane in the quiet-zone so that the  $u_z$ -component of the electric field is zero because of the symmetry.

The widths of the slots of the hologram depend on the frequency, the distance of the feed horn from the hologram and the function  $a(x', y')$ . In this case the widths of the slots vary between 5 and  $365 \mu\text{m}$  (or actually between 20 and  $360 \mu\text{m}$  because of the grid spacing in the calculation). Naturally, in this case the  $5 \mu\text{m}$  slot can not be fabricated. The effect of the fabrication error was simulated by changing the widths of the slots of the hologram in steps of  $40 \mu\text{m}$ . Figure 3 shows the ideal situation and situation where the slots are  $120 \mu\text{m}$  wider than in the ideal case. The amplitude and phase ripple inside the quiet-zone is  $0.3 \text{ dB}$  and  $1.3^\circ$  in the ideal case and  $0.7 \text{ dB}$  and  $3.0^\circ$  with the  $120 \mu\text{m}$  wider slots. Table 1 shows the resulting amplitude and phase ripple in the quiet-zone. In the figures and tables the quiet-zone is the area  $\rho \leq 50 \text{ mm}$ .

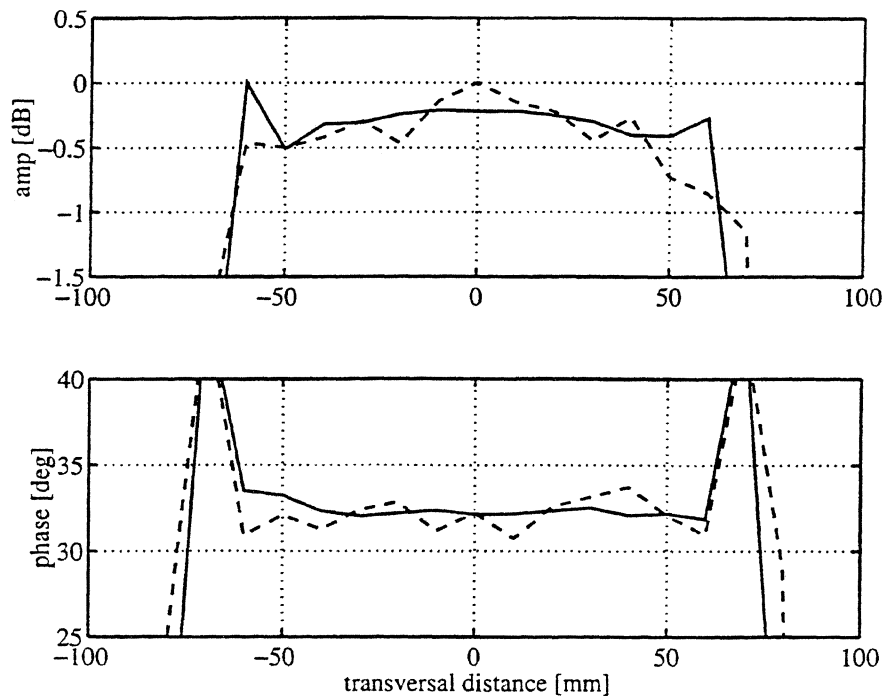


Figure 3. The amplitude and phase ripple in the quiet-zone: ideal case (solid line), slots are  $120 \mu\text{m}$  larger than in ideal case (dashed line).

Table 1. The amplitude and phase ripple in the quiet-zone, when the widths of the slots ( $w$ ) are changed.

$\Delta w$ [ $\mu\text{m}$ ]	amplitude ripple [dB]	phase ripple [deg]
-80	0.35	2.0
-40	0.25	2.0
0	0.30	1.3
40	0.40	1.0
80	0.55	2.0
120	0.70	3.0
160	1.0	4.0
200	1.3	5.0

The hologram which will be used in the testing of the Odin antenna will have to be fabricated by joining several pieces together. The displacement of the pieces has an effect on the field in the quiet-zone. This is simulated here by cutting the hologram from the middle into two pieces and displacing the parts 60, 100, 140 and 180  $\mu\text{m}$  from each other. The cut is in the  $x$ -direction as shown in Figure 4. The effect of the displacement ( $d$ ) is the inclination of amplitude and phase in quiet-zone in  $xz$ -plane. In  $y$ -direction there is no effects in the quiet-zone field. Figure 5 shows the worst case which was calculated (180  $\mu\text{m}$  displacement) compared to the ideal case. The results are presented in Table 2.

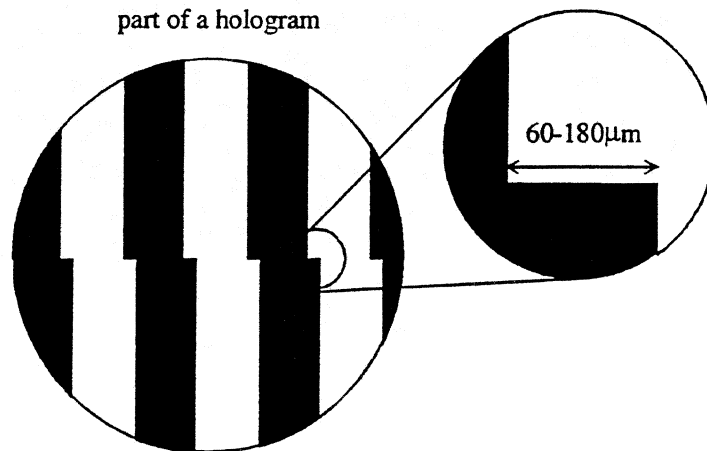


Figure 4. The displacement of the two different parts of the hologram.

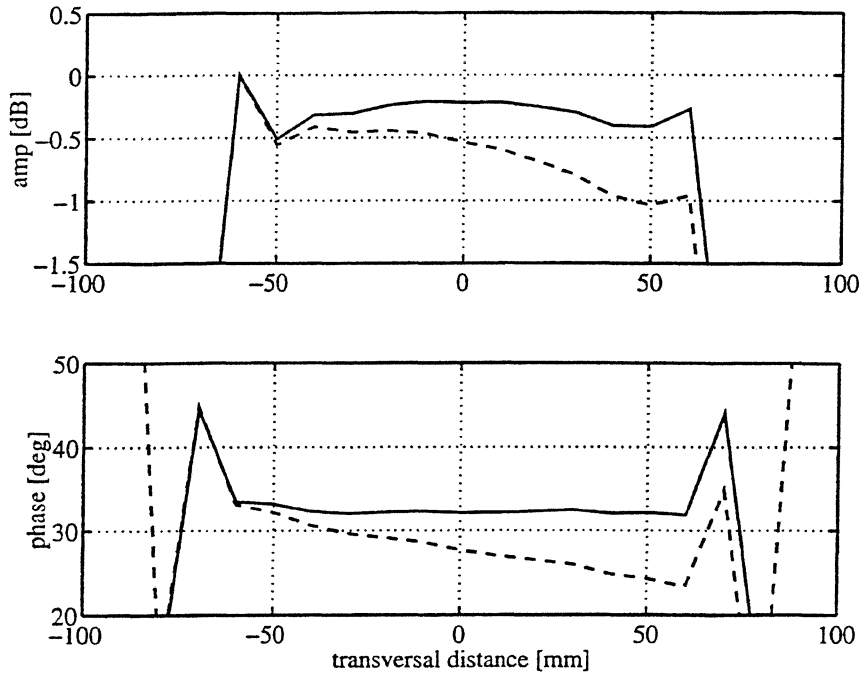


Figure 5. The amplitude and phase inclination in the quiet-zone caused by the displacement ( $d = 180 \mu\text{m}$ ) of the different parts of the hologram (dashed line). Solid line shows the situation without any displacement.

Table 2. The amplitude and phase inclination in the quiet-zone caused by the displacement ( $d$ ) of the different parts of the hologram.

$d$ [ $\mu\text{m}$ ]	amplitude inclination [dB]	phase inclination [deg]
0	0	0
60	0.05	4
100	0.2	5
140	0.4	6.5
180	0.6	8

Unavoidably, a hologram is a frequency dependent component, because the locations of the slots is determined by the phase of the incoming field. This was simulated by coding the hologram at 500 GHz and then calculating the field in the quiet-zone at different frequencies. The effect of the frequency change is the inclination of the phase front in  $xz$ -plane of the output field of the hologram. Figure 6 shows the situation when the frequency is changed from 500 GHz to 501 GHz. In Figure 6 the amplitude is almost unchanged and the phase changes  $77^\circ$  in the quiet-zone area, which means that instead of  $33^\circ$  the plane wave leaves the hologram in an angle of  $32.93^\circ$ . The angle can be calculated by using Equation (2). Similar results were obtained at 502 and 510 GHz. Only difference was the that the direction of the plane wave deviated more from  $33^\circ$ . The useful bandwidth of a hologram is case-specific, i.e.,

it depends on the actual center frequency and hologram size compared to the distance from the feed horn to the hologram. Logically, the field in  $y$ -direction is not affected by the frequency change.

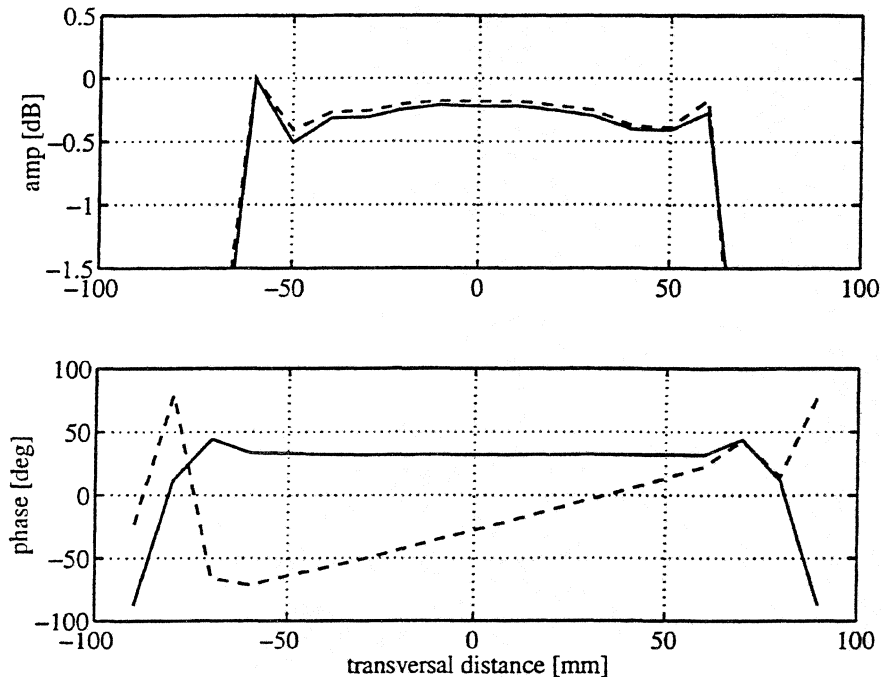


Figure 6. The field in the quiet-zone at frequencies 500 GHz (solid line) and 501 GHz (dashed line), when the hologram is coded at 500 GHz.

Main focus of this paper is on the hologram pattern errors parallel to the surface of the hologram. Obviously the quality of the quiet-zone is also effected by the flatness errors of the hologram, i.e. errors perpendicular to the surface of the hologram. The main advantage of an amplitude hologram is that inherently the surface errors of this structure have much less effect than those of a reflector. Figure 7 schematically enlightens this situation. The lower part of the figure, a hologram with surface error, shows that distances  $r_1$  and  $r_2$  have become shorter, but the shortening of these electrical lengths is partly compensated, because the incoming wave travels a longer way on the other side. Furthermore, because this is a transmission type of focusing element, we can have twice the surface error compared to the reflector. Due to this reasoning the planarity error is not assumed to be the main problem, but it will be studied more carefully during the project.



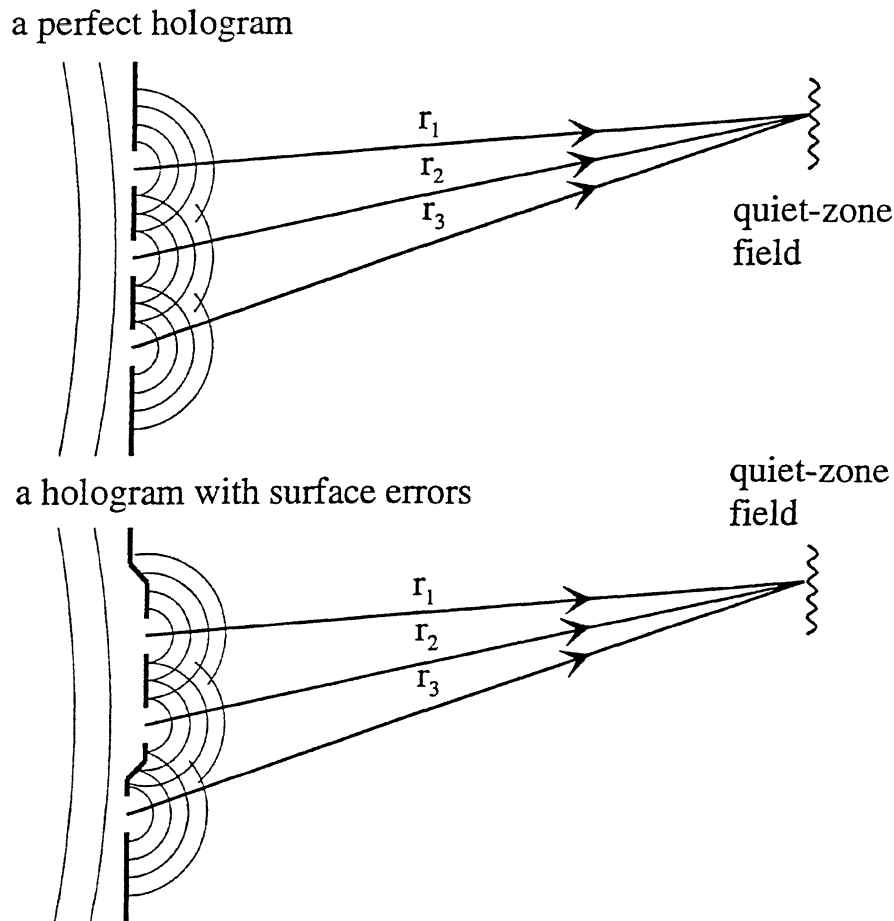


Figure 7. A side view of a perfect hologram and a hologram with surface errors.

## CONCLUSIONS

A hologram CATR is a new method for testing antennas at millimeter- and submillimeter wavelengths. According to the simulations carried out here for an ideal hologram it is possible to achieve a field in the quiet-zone which has a tolerable amplitude and phase ripple: 0.3 dB and 1.3 degrees. Due to fabrication errors the slots of the hologram are wider or narrower than in the ideal case, which increases the amplitude and phase ripple in the quiet-zone. However, with reasonable values of fabrication error the quality of the quiet-zone is not degraded decisively (Table 1). The effect of the displacement of the different parts of the hologram is the inclination of amplitude and phase in quiet-zone (Table 2). In the latter case the undesirable feature is the amplitude inclination, because together with the amplitude ripple caused by the fabrication error, the quality of the quiet-zone may degrade too much. The phase inclination caused by the displacement of the different parts of the hologram or a change in frequency is not a problem, because it only means that the plane wave leaves the hologram in a different angle than in the ideal case.

## ACKNOWLEDGEMENTS

The authors would like to thank Mr. Jyrki Louhi and Mr. Timo Haiko for useful discussions during this work.

## REFERENCES

- [1] Tuovinen, J., Vasara, A., Räsänen, A.: A new type of compact antenna test range. *Proceedings of the 22nd European Microwave Conference*, Espoo, 1992, pp. 503–508.
- [2] Aurinsalo, J., Karhu, S., Koivumäki, A., Pitkäaho, R., Lehto, A., Räsänen, A., Tolmunen, T., Tuovinen, J.: Test methods and ranges for testing the millimeter wave sounder of the Meteosat second generation satellites. Final report, ESTEC contract no. 7966/88/NL/PB(SC), March 1990.
- [3] Lee, W-H.: Computer-generated holograms: techniques and applications. In *Progress in Optics XVI*, Wolf, E., ed., North-Holland, 1978, pp. 119–232.
- [4] Burch, J., J.: A computer algorithm for the synthesis of spatial frequency filters. *Proceedings of the IEEE*, Vol. 55, 1967, pp. 599–601.
- [5] Vasara, A., Turunen, J., Friberg, A., T.: Realization of general nondiffracting beams with computer-generated holograms. *Journal of Optical Society of America A*, Vol. 6, 1989, pp. 1748–1754.
- [6] Kong, J., A.: *Electromagnetic Wave Theory*, John Wiley & Sons, New York, 1986, 696 p.
- [7] Hirvonen, T., Tuovinen, J., Räsänen, A.: Lens-type compact antenna test range at mm-waves. *Proceedings of the 21st European Microwave Conference*, Stuttgart, 1991, pp. 1079–1083.